IN-34

96731

P-47

NASA Contractor Report 4438

Distributed Acoustic Receptivity in Laminar Flow Control Configurations

Meelan Choudhari

NASA

NASA Contractor Report 4438

Distributed Acoustic Receptivity in Laminar Flow Control Configurations

Meelan Choudhari
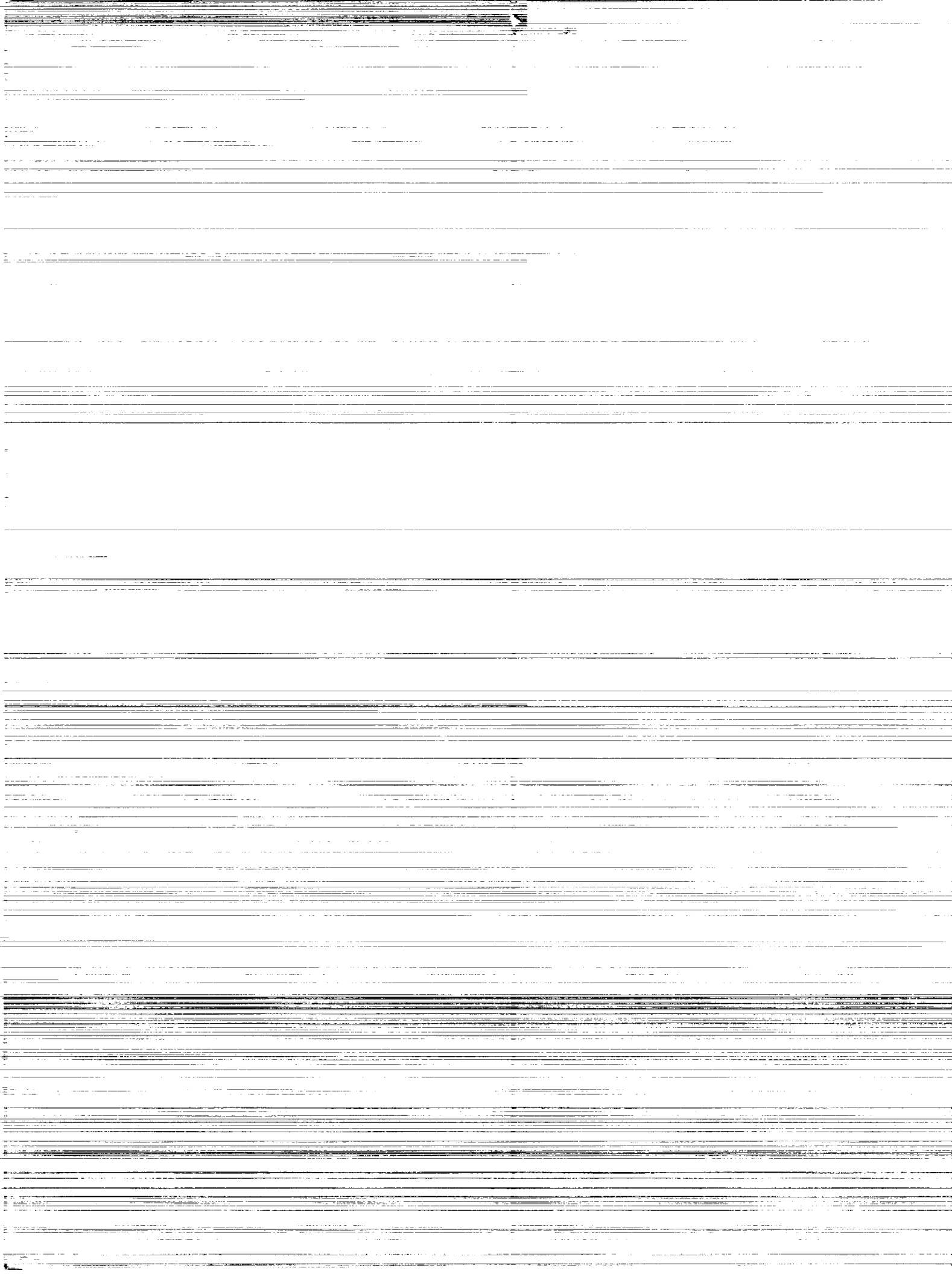*High Technology Corporation*
Hampton, Virginia

NASA

National Aeronautics and
Space Administration

Office of Management

Scientific and Technical
Information Program

1992

Distributed Acoustic Receptivity

in Laminar Flow Control Configurations

Meelan Choudhari

High Technology Corporation

Hampton, VA 23666

ABSTRACT

A model problem related to distributed receptivity to free-stream acoustic waves in laminar flow control (LFC) configurations is studied, within the Orr-Sommerfeld framework, by a suitable extension of the Goldstein-Ruban theory for receptivity due to localized disturbances on the airfoil surface. The results thus complement the earlier work on the receptivity produced by local variations in the surface suction and/or surface admittance. In particular, we show that the cumulative effect of the distributed receptivity can be substantially larger than that of a single, isolated suction strip or slot. Furthermore, even if the receptivity is spread out over very large distances, the most effective contributions come from a relatively short region in vicinity of the lower branch of the neutral stability curve. The length scale of this region is intermediate to that of the instability wave and the distance from the leading edge, being, in fact, a geometric mean of these two length scales. Finally, it is found that the receptivity is effectively dominated by a narrow band of Fourier components from the wall-suction and admittance distributions, roughly corresponding to a detuning of less than ten percent with respect to the neutral instability wavenumber at the frequency under consideration. The results suggest that the drop-off in receptivity magnitudes away from the resonant wavenumber is nearly independent of the frequency parameter.

1. INTRODUCTION

The importance of short-scale nonuniformities on the airfoil surface in making the boundary layer receptive to free-stream disturbances is now well established. Subsequent to the recent theoretical breakthrough by Goldstein[1] and Ruban[2], a number of problems involving different combinations of surface perturbation and free-stream disturbance have been studied in various flow regimes using both analytical and numerical techniques[3-17]. Additionally, experimental studies[18-21], albeit limited to low-speed flows thus far, have also contributed greatly to our understanding of these receptivity processes by inspiring or verifying the theories as well as by delineating the range of applicability of the different approximations used in theories. For reviews on different types of receptivity problems, see 22-26, and also Ref. 8 listed earlier. Most of this effort has focused on single, isolated surface inhomogeneities, with the exception of Crouch[5,6] who examined the nonlocalized receptivity due to a sinusoidal perturbation in the surface height. However, the conclusions of Refs. 5 and 6 concerning the magnitude of receptivity are contradictory to each other, and furthermore, the technique from these references appears suitable only for spatially homogeneous distributions containing a finite number of Fourier modes. On the other hand, Choudhari and Streett[4] have shown how the Goldstein-Ruban ideas can be used in combination with the local Green's function concept of Tam[27] for predicting the receptivity over longer regions by a simple extension of the results obtained for localized nonuniformities.

Here we take the route suggested by these latter investigators to study the acoustic receptivity due to an elongated region (i.e., much longer than an instability wavelength) of short-scale variations in the surface-porosity or suction-rate distribution. Suction is a common means to delay transition by stabilizing the laminar boundary layer, and a prefered choice for the design of a laminar flow control (LFC) system corresponds to suction distributed over a major portion of the airfoil surface through an array of porous strips[28-30]. Another option, which is nearly as effective, but is somewhat undesirable from a structural point of view, involves suction through a series of narrow surface slots in place of the porous strips. The main benefit of surface-suction is that it inhibits growth of the primary

2

instabilities[30-34], although there have also been some theoretical studies illustrating the use of suction for controlling the nonlinear stages of transition[35-37]. However, as shown by Kerschen and Choudhari[3], an undesirable side effect of these LFC configurations is an increased receptivity to unsteady free-stream disturbances which may offset the gain (in terms of reduced disturbance growth) to a certain extent. Thus, for a proper design of the LFC system, it is essential to understand the various routes, along with the associated magnitudes, of receptivity induced by the use of suction.

Kerschen and Choudhari[3] showed that the porous strip design can cause receptivity to acoustic type disturbances via two different mechanisms, the first being due to the short-scale mean flow gradients induced by variations in the wall suction, while the other (and perhaps more important) one is related to the accompanying variations in the admittance of the porous surface used for suction. They analyzed the acoustic receptivity in a localized area of short-scale variation, and were able to predict the influence of the width of a porous strip on the amplitude of the generated instability wave. In this paper, we consider the receptivity due to the entire suction system in the hope of shedding some light on the role of spacing between the adjacent suction strips/slots.

In Section 2, we describe how to calculate the receptivity due to surface non-uniformities spread over a region of arbitrary length. The advantage of the proposed Green's function technique is that it provides a convenient tool to analyze arbitrary nonlocalized geometries instead of just quasiperiodic distributions. Numerical results for several representative wall-suction or admittance distributions are presented in Section 3. Particular emphasis is placed on predicting the receptivity due to individual Fourier components of the distributed geometry. Conclusions derived from the analysis as well as numerics are presented in Section 4.

2. ANALYSIS

In this Section, we describe how the Goldstein-Ruban theory for receptivity induced by a local surface disturbance can be extended to distributed surface irregularities. However, before doing that, it will be useful to understand the physical ideas behind the generation of instability waves in a boundary-layer flow. Basically, the instability wave at any given frequency corresponds to the nearly periodic eigensolution of the small disturbance equations about the basic state of the quasi-parallel boundary layer. As discussed by Kerschen[8], the free-stream disturbances at this frequency have much different wavelengths than that of this eigensolution, and therefore, cannot excite the instability wave in a direct manner. The length-scale conversion or "tuning" process is brought about by the scattering of the forced unsteady motion, either at boundary inhomogeneities (such as variations in admittance or compliance of the airfoil surface) or in regions of rapidly varying (i.e., nonparallel) mean flow. The possible causes for mean flow non-parallelism include the leading edge as well as locally varying surface conditions in the downstream region, such as variations in the geometry, suction or blowing velocity, and surface temperature. In case of boundary layers which are also unstable to steady vortex type of instabilities, these surface disturbances act as sources of streamwise vorticity that gets amplified farther downstream[13,25]. Because of their broad variety as well as close proximity to the region of instability, the surface perturbations constitute a particularly important class of receptivity agents.

The first theoretical investigations in this class were by Goldstein[1] and Ruban[2], who used large Reynolds number asymptotics to show how an isolated surface distortion can interact with a free-stream acoustic wave to generate a Tollmien-Schlichting (T-S) wave in the region downstream. Since the role of all types of surface perturbations is essentially the same, namely, to provide the length scale required for coupling the free-stream and boundary-layer disturbances, the Goldstein-Ruban ideas are applicable, in principle, to this entire class of receptivity problems (see, for example, Refs. 3-17). In fact, Choudhari and Streett[4] and Federov *et al* (private communication) have shown how the Goldstein-Ruban

framework can also be extended to instability types other than T-S while simultaneously accounting for additional finite Reynolds number effects. It is this finite Reynolds-number implementation that will form the basis for the analysis of distributed receptivity to be presented in this Section. In principle, the problem of receptivity in an LFC configuration several wavelengths long could also have been tackled by an extension of the triple deck results for the localized case (Ref. 3). However, from our point of view, it merely seemed more convenient, and perhaps more accurate as well[4], to use the finite Reynolds number approach instead.

In this paper, we will restrict our attention to the low Mach number limit and, furthermore, assume the geometry to be a flat surface with specified admittance distribution; however, the speed and geometry limitations can be removed quite easily. The density and kinematic viscosity of the fluid are denoted by ρ^* and ν^*, respectively, and the incoming free stream is assumed to consist of a mean flow with speed U_∞^* plus a time harmonic acoustic perturbation with frequency ω^* and a streamwise velocity fluctuation of amplitude $u_{ac}^*(<< U_\infty^*)$. Since the acoustic wavelength is effectively infinite in the incompressible limit, the inviscid slip velocity above the surface is given by

$$u_\infty^* = U_\infty^* \left(1 + \epsilon_{fs} e^{-i\omega^* t^*} \right), \tag{2.1}$$

where $\epsilon_{fs}(<< 1)$ denotes the vanishingly small parameter associated with the free-stream disturbance amplitude u_{ac}^*/U_∞^*. The unsteady part of the slip velocity is also accompanied by a time harmonic, but spatially uniform pressure gradient of amplitude $-i\omega^*\rho^* u_{ac}^*$.

As discussed by Kerschen and Choudhari[3], these pressure fluctuations set up an unsteady mass flux across the porous surface, the distribution of which depends not only on the surface porosity, but also on the design of other components beneath the surface. However, the typical magnitude of this unsteady flux is quite small, since the porous surfaces used for LFC applications usually have rather small porosities. In addition, the design of the suction systems is such that the surface may be assumed to be "locally reacting", i.e., the unsteady flux at any location depends only upon the local details of the LFC configuration,

5

and can, therefore, be related to the incident pressure fluctuation by specifying the surface admittance distribution [†].

Since the absolute value of the pressure becomes irrelevant in the incompressible limit, it seems more appropriate to directly impose a short-scale distribution of the unsteady normal velocity at the wall instead of computing it indirectly by using the surface admittance distribution in conjunction with the specified acoustic amplitude. Thus, if the surface admittance $\beta^* \rho^* U_\infty^*$ is assumed to be of $O(\epsilon_w^{(2)})$ $(\epsilon_w^{(2)} << 1)$, then the corresponding unsteady velocity at the surface scaled by the acoustic particle velocity, v_a^*/u_{ac}^*, is also of $O(\epsilon_w^{(2)})$, and in addition, has the same spatial distribution as the surface admittance in the low Mach number limit. One may note that specifying the surface admittance, or equivalently, the unsteady surface velocity, has the advantage of rendering the results independent of the details of the suction system design beneath the surface; however, it may at times prove more useful to solve for the unsteady motion above and below the porous surface in a coupled manner. Pal et al[17] have recently used this approach to model the experiments of Wlezien et al[20] on receptivity near a porous suction strip with a large backing cavity underneath. Finally, it is also worth noting that in addition to modelling the wall admittance variation, the unsteady mass flux at the wall may also represent unsteady disturbances within the suction system, especially in designs with large suction slots.

Thus, we assume that the distributions of both the steady (suction/blowing) and unsteady (related to admittance) components of the normal velocity at the surface have weak but short-scale variations with respect to the streamwise coordinate in a region of arbitrary length located downstream of the leading edge (Figs. 1a-b). In more precise terms, these distributions are assumed to be given by

$$V_s^*(x^*) = \epsilon_w^{(1)} \ F^{(1)}(x^*)U_\infty^* \ , \tag{2.2a}$$

[†] The admittance of a surface is defined as the ratio, at the surface, of the (reduced) unsteady normal velocity to the fluctuating component of pressure.

and

$$v_a^*(x^*) = \epsilon_{fs}\, \epsilon_w^{(2)}\, F^{(2)}(x^*)\, U_\infty^*\, e^{-i\omega^* t^*}\,, \tag{2.2b}$$

where the nondimensional parameters $\epsilon_w^{(1)}$ and $\epsilon_w^{(2)}$ characterize the small magnitudes of the wall suction-velocity and wall admittance, respectively, while functions $F^{(1)}(x^*)$ and $F^{(2)}(x^*)$ denote the (normalized) distributions of these quantities along the streamwise direction. As mentioned previously, the long wavelength acoustic wave can excite the boundary-layer instabilities via an interaction with the surface disturbances only if the length scale of the latter becomes comparable to the instability wavelength in at least a part of the entire region. However, other than this condition, the distribution functions $F^{(1)}(x^*)$ and $F^{(2)}(x^*)$ can assume any arbitrary form during this analysis. Both of the above constraints relating to the magnitude and length scale of the $V_s^*(x^*)$ and $v_a^*(x^*)$ distributions are consistent with the typical designs of LFC systems.

In order to distinguish between the dependence on the longer length scale corresponding to the slow growth of the unperturbed boundary layer and the shorter length scale of the imposed surface disturbance, we introduce the streamwise coordinates $x = x^*/\ell^*$ and $X = x^*/L^*$, respectively. Here x^* denotes the distance from the leading edge with the reference length ℓ^* being chosen so as to make $x = O(1)$ (Fig. 1b). The Reynolds number $R_{\ell^*}\ (= U_\infty^*\ell^*/\nu^*)$ is assumed to be sufficiently large so the stability of the unperturbed mean flow is governed by the classical, quasi-parallel theory. The shorter length scale L^* represents a typical instability wavelength, which is asymptoticaly much larger than the thickness of the boundary layer. However, it is traditional in the classical stability theory to use the same shorter length scale for both the streamwise and wall-normal directions, and accordingly, we will identify L^* with a typical boundary-layer thickness, and define the nondimensional wall-normal coordinate as $Y = y^*/L^*$ and the streamfunction as $\psi = \psi^*/(U_\infty^* L^*)$. Similarly, the nondimensional time t and frequency ω will be assumed to have been normalized by L^*/U_∞^* and its inverse, respectively. Note that the precise definition of the reference length scales will be left open for the time being since doing so will prove convenient for subsequent manipulations.

The streamfunctions $\psi^{(j)}$, $j = 1, 2$, are governed by the two-dimensional Navier-Stokes equation,

$$\frac{\partial \nabla^2 \psi^{(j)}}{\partial t} + \frac{\partial \psi^{(j)}}{\partial Y} \frac{\partial \nabla^2 \psi^{(j)}}{\partial X} - \frac{\partial \psi^{(j)}}{\partial X} \frac{\partial^3 \psi^{(j)}}{\partial Y^3} - \frac{1}{R_{\delta^*}} \nabla^4 \psi^{(j)} = 0 \; , \qquad (2.3)$$

where the suffix j has been introduced to distinguish between the receptivity due to wall suction ($j = 1$) and the wall admittance ($j = 2$) variations. Accompanying the differential equation (2.3) are the inhomogeneous surface boundary conditions

$$\frac{\partial \psi^{(1)}(X, 0)}{\partial X} = \epsilon_w^{(1)} F^{(1)}(X) \; , \qquad (2.4a)$$

and

$$\frac{\partial \psi^{(2)}(X, 0)}{\partial X} = \epsilon_{fs} \epsilon_w^{(2)} F^{(2)}(X) \, e^{-i\omega t} \; , \qquad (2.4b)$$

corresponding, respectively, to specified distributions of the mean and unsteady components of the normal velocity at the wall. Since the surface porosities are assumed to be small, motion at the surface location is nearly in the normal direction, and, therefore, both $\psi^{(1)}$ and $\psi^{(2)}$ can be assumed to satisfy the no-slip condition at $Y = 0$. Finally, each of these streamfunctions needs to match the imposed free-stream behaviour (2.1) far away from the wall.

This completes the formulation of the problem. In the remaining part of this Section, we describe how the small-amplitude assumption concerning the surface and free-stream perturbations can be utilized in determining the instability motion generated in both cases. This analysis hinges heavily upon the earlier asymptotic analyses[1−3], as well as on the finite Reynolds number adaptations thereof, for a localized receptivity problem. Therefore, only a brief sketch of the derivation will be given here, leaving the interested reader to find the details in the above mentioned references.

For the doubly-linearized receptivity problems (i.e., both $\epsilon_w^{(j)}$, $\epsilon_{fs} \ll 1$), one can expand the flow variables in the form of a dual perturbation series. Such a series was used originally by Goldstein and Ruban (and subsequently in Refs. 3, 7, 8, 10 − 12, 16, 26),

8

to obtain closed form solutions to the localized receptivity problem via a rational (triple deck) treatment of the finite Reynolds number effects and, more recently, in Refs. 4, 5, 15 and 17, to obtain numerical solutions in the framework of the (nonasymptotic) classical stability equations. The streamfunctions $\psi^{(j)}$ can thus be written in the form

$$\psi^{(j)} = \Psi_0(x,Y) + \delta_{1,j}\, \epsilon_w^{(j)}\Psi_1^{(j)}(X,Y) + \epsilon_{fs}\psi_0(x,Y)e^{-i\omega t}$$

$$+ \epsilon_{fs}\epsilon_w^{(j)}\psi_1^{(j)}(X,Y)e^{-i\omega t} + O(\epsilon_{fs}^2, {\epsilon_w^{(j)}}^2, \epsilon_l, R_{\delta^*}^{-1}) , \tag{2.5}$$

where the factor $\delta_{1,j}$ is equal to unity for $j = 1$, and zero otherwise. Each term in this perturbation sequence represents a unique combination of spatial and temporal scales related to the physical origin of this perturbation; the dichotomy of streamwise length scales is symbolized by using the suffixes 0 or 1, while the steady and unsteady components of motion are distinguished by using upper and lower case letters, respectively. The zeroth-order term Ψ_0 represents the streamfunction corresponding to the mean boundary-layer flow which would exist in the absence of both the wall-suction and the free-stream disturbance. Thus, it is steady, and in the streamwise direction only depends upon the slow coordinate x. For the flat-plate geometry under consideration, it is given by the self-similar Blasius solution. The quantities $\Psi_1^{(1)}$ and ψ_0 denote the first-order perturbations to this base flow due to the steady surface suction and the unsteady free-stream disturbance, respectively. Accordingly, $\Psi_1^{(1)}$ is a steady perturbation, but varies on the faster streamwise scale X of the wall suction distribution, while ψ_0 represents the acoustic boundary-layer motion and, therefore, varies on the longer x scale only. In fact, to the leading order in Reynolds number expansion, it is given by the x-independent Stokes shear wave solution, which also turns out to be sufficiently accurate for our purpose. One may note that, in order to generate an instability wave, it is necessary to excite a boundary-layer motion having shorter scales in both space and time dimensions. The first term in the perturbation series which posseses this required characteristic is tae $O(\epsilon_{fs}\, \epsilon_w^{(j)})$ term produced by the interaction of the $O(\epsilon_w^{(j)})$ and $O(\epsilon_{fs})$ perturbations. As pointed out by Kerschen and Choudhari[3], in the case of suction-induced receptivity, his $O(\epsilon_{fs}\, \epsilon_w^{(j)})$ term corresponds

to a temporal modulation of the short-scale mean flow gradients induced by wall suction variation, while in the wall-admittance problem, it represents the scattering of the incident acoustic motion by the $O(\epsilon_w^{(2)})$ variations in surface admittance.

Our objective here is to solve the receptivity problem and not to obtain the complete second-order asymptotic expansion for the boundary-layer motion. To obtain the leading-order solution for the receptivity problem, it is sufficient to solve for just the $O(\epsilon_{fs}\,\epsilon_w^{(j)})$ term and ignore the other second-order terms, namely, $O(\epsilon_{fs}^2)$ and $O(\epsilon_w^{(j)^2})$, since they do not possess the desired combination of spatio-temporal scales. Moreover, since we are only interested in the part of $\psi_1^{(j)}$ which corresponds to the instability wave, it is not even necessary to obtain a complete solution for the $O(\epsilon_{fs}\,\epsilon_w^{(j)})$ term. The way we accomplish this limited objective is to first isolate the T-S wave produced in each local region and then sum over all these contributions to obtain the total instability amplitude at any given location. While carrying out this integration process, we also account for the changes in phase and amplitude of the instability wave in travelling from its source location to the observation point. The weakly-nonparallel effects due to streamwise divergence of the base flow are unimportant in calculating the local contribution, but they can become significant during propagation if distances comparable to the body length scale (ℓ^*) are involved. However, these effects can be accomodated *post-facto* by using results from standard weakly-nonparallel theory[38].

Substituting the perturbation expansion (2.5) into (2.3), collecting terms of $O(\epsilon_w^{(j)}\epsilon_{fs})$, and exploiting the disparity of length scales between the slowly-evolving solutions (Ψ_0 and ψ_0) and the short-scale motion of interest here, we obtain the usual equation governing the propagation of unsteady disturbances in a parallel shear flow,

$$\frac{\partial \nabla^2 \psi_1^{(j)}}{\partial t} + \frac{\partial \Psi_0}{\partial Y}\frac{\partial \nabla^2 \psi_1^{(j)}}{\partial X} - \frac{\partial^3 \Psi_0}{\partial Y^3}\frac{\partial \psi_1^{(j)}}{\partial X} - \frac{1}{R_{\delta^*}}\nabla^4 \psi^{(j)} + O(\epsilon_{\ell^*})$$

$$= \delta_{1,j}\left(-\frac{\partial \psi_0}{\partial Y}\frac{\partial \nabla^2 \Psi_1^{(1)}}{\partial X} + \frac{\partial^3 \psi_0}{\partial Y^3}\frac{\partial \Psi_1^{(1)}}{\partial X}\right) , \qquad (2.6a)$$

along with a surface boundary condition that is nonzero only for $j = 2$,

$$\frac{\partial \psi_1^{(j)}(X,0)}{\partial X} = F^{(2)}(X) , \qquad (2.6b)$$

10

the remaining boundary conditions being all homogeneous. The neglected $O(\epsilon_{\ell^*})$ terms on the left hand side represent the $O(L^*/\ell^*)$ weakly-nonparallel terms related to the slow growth of the unperturbed mean boundary layer. The neglect of these terms is justified, at this stage, only on the basis of the historical success of the quasiparallel approximation in producing results which are in satisfactory agreement with the experiments as well as direct numerical simulations. As we show later, the net receptivity is effectively concentrated in a relatively short region with a length scale that is intermediate between the instability wavelength and the distance from the leading edge. Hence, it is also possible to justify the quasiparallel approximation in this problem on a rational basis. Moreover, as alluded to above, the nonparallel effects can also be incorporated into the resulting equations in an *a posteriori* manner.

As seen from (2.6), $\psi_1^{(1)}$ satisfies an inhomogeneous differential equation with a source term arising from the interaction of the short-scale mean flow perturbation $\Psi_1^{(1)}$ with the leading unsteady perturbation ψ_0. On the other hand, since the motion corresponding to $\psi_1^{(2)}$ is driven only by the forcing at the boundary, it seems convenient to illustrate the solution procedure just for this case, and then quote the final result for the wall-suction problem. Thus, from now on we will suppress the effects of steady surface suction and only solve for the streamfunction $\psi_1^{(2)}$. We will first obtain the solution for $\psi_1^{(2)}$ (actually the T-S wave part of it) by a formal Green's function technique which was first used by Tam[26] in a similar context, and subsequently show how the same solution could also have been obtained by generalizing the solution obtained for a localized receptivity problem. In order to obtain the Green's function $G^{(2)}(X, Y; \omega | X_s)$, set $F^{(2)}(X) = \delta(X - X_s)$ where the subscript s denotes the position of the source. In order to obtain the instability component of the streamfunction $\psi^{(2)}$, it is again sufficient to solve for just the part of the Green's function G which corresponds to the T-S wave produced by the point source at $X = X_s$. This can be done quite easily by extracting the residue of the pole, corresponding to the local T-S wavenumber, of the Fourier transform of $G^{(j)}$ with respect to the fast streamwise variable X. After introducing the local coordinate $\xi = X - X_s$ and the Fourier transform

$$\bar{G}^{(2)}(\alpha, Y) = \frac{1}{\sqrt{2\pi}} \int_{-\infty}^{\infty} e^{-i\alpha\xi} G^{(2)}(\xi, Y) \, d\xi \quad , \tag{2.7}$$

11

equation (2.6) reduces to the Orr-Sommerfeld (O-S) equation

$$-i\omega(\frac{d^2}{dY^2} - \alpha^2)\bar{G}^{(2)} + i\alpha\hat{\Psi}_0'(\frac{d^2}{dY^2} - \alpha^2)\bar{G}^{(2)} - i\alpha\hat{\Psi}_0'''\bar{G}^{(2)} - \frac{1}{R_{\delta*}}(\frac{d^2}{dY^2} - \alpha^2)^2\bar{G}^{(2)} = 0 \ ,$$

(2.8a)

subject to

$$i\alpha\bar{G}^{(2)}(\alpha,0) = 1/\sqrt{2\pi} \ ,$$

(2.8b)

leading to the following expression for the T-S wave produced by the point source at $X = X_s$:

$$G_{qTS}^{(2)}(X,Y;\omega|X_s) = \frac{1}{\sqrt{2\pi}} E_q(Y;\omega,x) \Lambda^{(2)}(\omega,x_s) e^{i[\Theta_{TS}(X)-\Theta_{TS}(X_s)]} H(X - X_s) \ ,$$

(2.9a)

Here $E_q(Y; \omega, x)$ denotes the (appropriately normalized) instability wave eigenfunction for the physical quantity denoted by q, while $\Lambda^{(2)}$ represents the normalized initial amplitude (i.e., at the source location) of the fluctuation in q, determined numerically as the residue contribution corresponding to the pole of $\bar{G}^{(2)}$ at the local T-S wavenumber $\alpha = \alpha_{TS}(x_s)$. In this paper, we will assume the eigenfunctions for different flow variables to have been normalized to make the maximum of the streamwise velocity fluctuation across the boundary layer equal to unity. The spatial phase Θ_{TS} of the generated instability wave is given by the indefinite integral over the slowly varying wavenumber,

$$\Theta_{TS}(X) = \int^X \alpha_{TS}(x) \, dX \ .$$

(2.9b)

We would like to point out that the Green's function problem (2.8a,b) is mathematically identical to the vibrating-ribbon problem first analyzed by Gaster[39], and subsequently by others in Refs. 40-41. Moreover, G_{qTS} is also equivalent to a special case (corresponding to a point disturbance) of the "outer" solution for the problem of receptivity due to a local region of wall-admittance variation (Refs. 3,4). Thus, the function $\Lambda^{(2)}$ in (2.9a) is identical to the "efficiency function" of Ref. 4, apart from a scaling factor related to the particular choice for the length scale L^*. The $\Lambda^{(j)}$ function characterizes the intrinsic efficiency of any

localized receptivity process, being dependent only on the types of free-stream disturbance and surface non-uniformity, along with the mean boundary-layer profile.

Using (2.9a), it is easy to see that the T-S wave part of the total unsteady motion is given by the integral

$$q_{TS}^{(2)} = \frac{1}{\sqrt{2\pi}} E_q(Y; \omega, x) e^{i\Theta(X)} \int^X \Lambda^{(2)}(\omega, x_s) F^{(2)}(X_s) e^{-i\Theta(X_s)} H(X - X_s) dX_s. \quad (2.10)$$

It is then immediately obvious that this solution could also have been obtained from the localized solution

$$q_{TS}^{(2)} = \frac{1}{\sqrt{2\pi}} E_q(Y, x; f) \Lambda^{(2)}(\omega, x) e^{i\alpha_{TS} X} \int_{X_i}^{X_f} F^{(2)}(X_s) e^{-i\alpha_{TS} X_s} dX_s, \quad (2.11)$$

X_i and X_f being the extremities of the local inhomogeneity, by letting the boundary-layer properties, i.e., the instability wavenumber α_{TS} and the efficiency function $\Lambda^{(2)}$, vary over the length of the receptivity region. Note that the Green's function technique fails in the wall-suction case since the inhomogeneity there depends on both the streamwise and wall-normal coordinate (2.6a). However, the generalization of the localized results in the above sense is still valid, thus enabling us to relate the T-S wave amplitude directly to the steady suction distribution via the efficiency function $\Lambda^{(1)}$ obtained for the localized problem.

The above results establish a clear connection between the localized and nonlocalized receptivity problems; not only is the underlying physical mechanism the same in these problems, but in fact, the same general equation (namely, 2.10) can be used to determine the instability wave amplitude, given the streamwise distribution of the surface non-uniformity. This relationship between the two types of problems was also discussed by Nishioka and Morkovin[22] in their review of boundary-layer receptivity. For most practical purposes, the only major difference between the localized and nonlocalized receptivities corresponds to the length of the integration domain, which, in the latter case, is much larger than the length scale over which the integrand varies. As a result, it would seem that the distributed receptivity problems need to be studied separately for each geometry of

interest, since it is not possible to separate the influence of surface geometry from that of an intrinsic efficiency function, $\Lambda^{(j)}$, as in the localized case (2.11). However, later results will show that, since the receptivity is still concentrated in a relatively short region compared to the length scale (ℓ^*) over which $\Lambda^{(j)}$ varies significantly, decoupling of the above type is still possible. Furthermore, Eq. (2.10) also suggests that due to the additive effect over a large number of wavelengths, the receptivity due to distributed nonuniformities could become significantly larger than that for a single, isolated nonuniformity. The extent of this increase is crucially dependent upon the relative phase and magnitude of the contributions from different receptivity locations. In this context, it is worth noting the resemblance between the integral in (2.10) with those arising in wavepacket problems, or to be more precise, in studies of spatial wave patterns produced by time harmonic point sources. Of course, physically, the difference between the two types of problems is that, in the wave pattern case, the value of the integral is determined by the interference between different wavenumber components emanating from the same spatial location, while in the present problem, the resultant motion is determined by an interference between waves of the same type (the T-S mode) but produced by a sequence of sources, the phase variation among which is decided by the spatial distribution $F^{(j)}$ of the surface nonuniformity. Finally, it is also possible to draw an analogy between the present problem with diffraction problems in optics. The solutions (2.9), (2.11) and (2.10) are roughly analogous to the electromagnetic field generated by a compact source and that in a Fraunhoffer and in a Fresnel region, respectively.

For computational purposes, it is more convenient to express the integral solution (2.10) in terms of the local Reynolds number $R = R_{x^*}^{-1/2}$. Hence, identifying the shorter length scale L^* with the local boundary-layer scale, $R_{x^*}^{-1/2} x^*$, and recognizing the invariance of the right hand side of (2.10) with respect to the choice of the length scale, we obtain the equation

$$q_{TS}^{(j)} = \sqrt{\frac{2}{\pi}} \, E_q(Y; \omega, R) \, e^{i\Theta_{TS}(R)} \int^{R} \Lambda^{(j)}(\omega, R_s) \, F^{(j)}(R_s) \, e^{-i\Theta_{TS}(R_s)} \, H(R - R_s) \, dR_s,$$

$$(2.12)$$

14

where $\Lambda^{(j)}$ now denotes the efficiency function based on the local length scale, as obtained, for instance, in studies of localized receptivity problems[3,4]. All quantities in (2.12) other than the instability phase Θ_{TS} and the geometry function $F^{(j)}$ are slowly-varying functions of the Reynolds number R. To show the variation of the efficiency function, $\Lambda^{(j)}$, with R, its magnitude is plotted for both the wall-suction and wall-admittance problems in Figs. 2a and 2b, respectively. So that the reader may have an idea about the variation of the efficiency function, $\Lambda^{(j)}$, with R, we have plotted its magnitude for both the wall-suction and wall-admittance problems in Figs. 2a and 2b, respectively. For reference, the lower and upper branch locations at each frequency are also indicated by open and filled circles, respectively, in both these figures. Since the streamwise velocity perturbation is of primary interest in low-speed flows, the ordinate in these figures corresponds to the choice $q = u$ in $\Lambda^{(j)}$. For this same reason, all subsequent results in this paper will also be based on the streamwise velocity perturbation associated with the generated instability motion.

By differentiating with respect to R, Eq. (2.12) can also be converted to a wave amplitude equation similar to that obtained by Tam[27],

$$\frac{\partial u_{TS}^{(j)}}{\partial R} = i \frac{\partial \Theta_{TS}}{\partial R} u_{TS}^{(j)} + \sqrt{\frac{2}{\pi}} \Lambda^{(j)} F^{(j)} + O(\epsilon_\ell), \qquad (2.13)$$

where $u_{TS}^{(j)}$ denotes the maximum of the streamwise velocity perturbation across the boundary layer at station R, while $\frac{\partial \Theta_{TS}}{\partial R}$ represents twice the slowly-varying instability wavenumber α_{TS}, and the $O(\epsilon_\ell)$ terms are again related to the weak non-parallelism of the base flow. The homogeneous solution of this amplitude equation corresponds to the nearly-periodic T-S motion which is generated wherever the local spectrum of the geometry function $F^{(j)}(R)$ overlaps with the T-S mode. As seen from Eq. (2.13), when the receptivity occurs continuously over a large number of instability wavelengths, the change in the wave amplitude at any station is due to a combined effect of the local amplification of the instability waves generated upstream of the present location and the external input due to local receptivity. As pointed out by Tam[27], the relative contribution from the two different inputs depends on the local amplitude of the instability wave. In the region where the receptivity begins,

it is obvious that the local rate of change will be dominated by the contribution from the external disturbance. However, when the instability amplitude has reached a sufficiently large magnitude, this contribution becomes much smaller compared to the local amplification due to transfer of energy from the mean flow. Hence, one can expect that as the location corresponding to the upper branch of the neutral stability curve is approached, the amplitude evolution curve will asymptote to that of a pure T-S wave eigensolution. Of course, in the immediate vicinity of the upper branch location, where the instability growth rates are very small, the rate of change in the amplitude is again dominated by the external input. However, the streamwise extent of this region, which now corresponds to the shift in the neutral location (i.e., where the disturbance amplitude is stationary), is rather small, being inversely proportional to the amplitude in this region. Thus, unless the dominant surface nonuniformities occur far downstream of the lower branch, a case which is not of much practical interest, one may assume that the maximum instability amplitude is practically the same as the amplitude at the theoretical neutral location.

Since the maximum instability amplitude is most relevant to an "amplitude" criterion used for transition prediction, it may be viewed as a global measure of the generated instability motion in a distributed-receptivity problem. Moreover, in order to separate the receptivity, *per se*, from the linear amplification stage, one could divide this maximum amplitude by the amplification factor between the two neutral locations to obtain an "effective coupling coefficient", $C^{(j)}$, at the lower branch location, i.e., before the beginning of the linear amplification stage. Note that a local coupling coefficient[1,27] relates the output of the receptivity process, i.e., the amplitude of the generated instability wave, to its input, i.e. the free-stream disturbance amplitude. Since we are considering weak surface disturbances here, it also varies linearly with the amplitude of the surface disturbance, and will, therefore, be assumed to be normalized by this latter input as well. The effective coupling coefficient, $C^{(j)}$, corresponds to the local coupling coefficient for an equivalent, but ficticious localized mechanism which has all its receptivity lumped together at the lower branch station, in the sense of leading to the same maximum instability amplitude. From

16

this perspective, one may also gauge the development of the entire receptivity process by examining the cumulative contribution to this effective coupling coefficient as a function of the local Reynolds number.

3. NUMERICAL RESULTS

In this Section, we present numerical solutions to the wave amplitude equation (2.13) for some representative distributions of the wall suction velocity and the wall admittance. The first type of distribution considered below is a single region of uniform suction/admittance distribution, i.e., the isolated suction strip case analyzed in Ref. 3 using localized receptivity analysis. Of course, multiple strip configurations are more relevant to LFC[29], and these are analyzed next. Reed and Nayfeh[33] examined theoretically a number of multiple strip configurations involving different combinations of parameters such as the total number of strips, spacing between the adjacent strips, and finally, variation in the amount of suction applied through each strip. These investigators also carried out an optimization study in order to determine the configuration which has the most beneficial effect on the stability of the dangerous frequency components. Here, we make an effort to complement that study by examining what effect the various configurations have on the receptivity stage. Finally, we consider in detail the case of uniformly spaced porous strips, where it is possible to arrive at some general conclusions regarding the distributed receptivity problem, by separately analyzing the receptivity due to each Fourier harmonic of the periodic distribution. In fact, it is also possible to obtain closed-form analytical solutions for this case which provide extra insight into the distinctive features of the distributed-receptivity problems; see, for instance, Ref. 42, where we examine this case in connection with random surface inhomogeneities. In this paper, we will content ourselves with presenting a more physical discussion based on the theory of Ref. 42, which will serve as a background for the understanding and interpretation of the subsequent numerical results.

Let us begin with the case of a single, isolated suction strip with a uniform suction/admittance distribution. Figure 3a shows the effective coupling coefficient for both

mechanisms plotted against the width of this strip for a frequency parameter corresponding to f $(\equiv \omega^* \nu^* / U_\infty^{*2})$ = 20 x 10^{-6}, where we have assumed the suction strip to be centered on the lower branch location at this frequency. The absissca w in this graph corresponds to the strip width normalized by the local instability wavelength, whereas the ordinate has been scaled by the coupling coefficient in the narrow strip limit, $w \rightarrow 0$. While varying the width of the suction strip, we have assumed the level of the surface admittance to be fixed. However, the suction velocity is varied with w so as to keep the total mass flow rate constant, since it is the latter quantity which determines the overall reduction in the growth of the instability wave. The results from the present (nonlocalized) theory are shown by solid curves in Fig. 3a, while the broken line curves represent results from the localized analysis in Ref. 3.

The receptivity in discrete configurations is concentrated at the points of discontinuity (Fig. 3b), and, hence, the generated instability motion corresponds to a superposition of the T-S waves generated at each end of the strip. Since both of these waves have identical amplitudes in a localized analysis, it is obvious that their mutual interference will lead to a complete cancellation of each other for integer values of w, whereas a mutual reinforcement will result for $w = n + 1/2$ [3]. In the non-localized analysis, variation of boundary-layer properties between the two ends alters this simple scenario by affecting both the relative amplitude and phase of the T-S waves generated at the two ends of the strip. In the particular case shown in Fig. 3a, $\Lambda^{(1)}$ and $\Lambda^{(2)}$ decrease in magnitude by approximately 9% and 23%, respectively, across the two ends of the strip when $w = 5$. However, the effect of these variations appears to be pronounced only in the vicinity of the extrema of the coupling coefficient curve, especially for $w > 2.0$. Of course, such wide strips are not very relevant to LFC, except possibly at rather high frequencies where the instability wavelength is quite small. Nevertheless, this simple example serves to illustrate how variations in boundary-layer properties across the region of receptivity start to become significant as this region becomes elongated in its streamwise extent.

Next, consider the wall-suction and wall-admittance distributions corresponding to multiple strip configurations. The objective here is to assess the effects of large-scale non-uniformities due to the concentration of suction in certain parts of the airfoil chord. The different cases examined as part of this study are listed in Table 1, and will be summarized now. Note that in their stability related investigation, Reed and Nayfeh only considered the effects of applying suction between the two neutral branches. However, such may not always be the case. In fact, the hybrid LFC approach combines the use of suction in the leading edge region with a favorable pressure gradient in the mid-chord region for reducing the growth of boundary-layer instabilities[29]. Hence, we examined the receptivity due to uniform suction applied through regularly-spaced suction strips in both the front and/or mid-chord regions (cases i-iii in Table 1). Figure 4 shows the cumulative variation in the effective coupling coefficient for these three cases. As one can see from case iii, the receptivity is distributed quite symmetrically on both sides of the lower branch station, with the strips closer to the neutral station being more effective than those away from it. Thus, the contribution to $|C^{(j)}|$ from strips 13 and 14 (which are closest to $R_{l.b.}$) is $O(100)$ in this case, while that of number 1 and 24 is only about $O(1)$ or smaller. This is to be expected since the instability waves generated close to the lower branch location can undergo the highest possible amplification before reaching the upper branch.

Reed and Nayfeh also studied the effects of non-uniformly distributed suction, and found that increased amounts of suction in the vicinity of the two neutral branches was particularly beneficial for reducing the instability amplification (Figs. 14-16 vs. Figs. 20-22 in Ref. 33). On the other hand, a configuration involving twice the amount of suction in the middle third of the strips was found to be sub-optimal (Figs. 17-19 in Ref. 33). In contrast to this, we found that increasing the amount of suction by 20% in the two neutral zones (while reducing the suction in the middle third of the strips by 40% in order to keep the total suction the same) increased $C^{(1)}$ by approximately 20% (case iv) as compared to the case of uniform distribution, (ii). On the other hand, the suboptimal configuration from the viewpoint of stability decreased the receptivity by 25% (case v). This behaviour

suggests that the requirements for optimizing the receptivity and stability processes may at times counter to each other. Note that the gains obtained by optimizing the suction distribution for reduced amplification are not overly spectacular corresponding to reduction of about 3-4% in the N-factor or equivalently, instability amplitudes which are smaller by a factor of 20-30%. Since the results above indicate that comparable benefits may also be expected from the optimization of the receptivity stage, serious consideration should be given to the question of combined optimization methods whenever the overall receptivity is dominated by the suction/admittance-induced receptivity.

Before moving on to the next case, we would like to point out that the suction configuration used by Reed and Nayfeh[33] involved 5/8″ wide strips which were spaced rather far apart (4.5″). Since we felt that this set of dimensions represented too small a ratio for the strip width to the spacing between the strips, we chose a value of 0.6 for this ratio in the above calculations, and assumed the strip spacing to be equal to the neutral T-S wavelength at the frequency being considered ($f = 20 \times 10^{-6}$). The strip spacings in actual designs are likely to be even smaller than the T-S wavelength, but the above conclusions concerning the influence of the different types of spatially inhomogeneous distributions are not likely to depend upon either the width of the strips or the spacing between them. The influence of strip spacing on the receptivity due to wall suction/admittance distributions that are homogeneous on the longer length scale of the receptivity process will be analyzed in the remaining part of this Section.

Since distributions of this type can be analyzed in terms of their individual Fourier harmonics, we now consider spatial distributions of the form

$$F^{(j)} = e^{i\theta_w(R)} \quad \text{where} \quad \frac{d\theta_w}{dR} = 2\alpha_w(R) = 4\pi\frac{R}{R_{\lambda_w^*}} \ , \qquad (2.14)$$

$R_{\lambda_w^*}$ being the Reynolds number based on the dimensional wavelength $\lambda_w^*(= 2\pi/\alpha_w^*)$ of the surface distribution, while α_w denotes the dimensionless wavenumber based on the slowly-varying local length scale, L^*. The distributions given by (2.14) serve as models for designs involving regularly-spaced suction strips (with uniform suction levels) which

extend over a significant portion of the airfoil chord. Discrete distributions of this type can essentially be viewed as a continuous area suction (which does not produce any receptivity) with oscillatory components corresponding to various harmonics which can be analyzed independently of each other.

Now consider the integral form of the solution (2.10) for the above case,

$$q_{TS}^{(j)} = \sqrt{\frac{2}{\pi}}\, E_q(Y; \omega, R)\, e^{2i \int^R \alpha_{TS} dR} \int^R \Lambda^{(j)}(\omega, R_s)\, e^{2i \int^{R_s} (\alpha_w - \alpha_{TS}) d\tilde{R}}\, dR_s, \quad (2.15)$$

which shows that in regions where the forcing wavenumber α_w is significantly different from the eigenmode wavenumber α_{TS}, the integrand oscillates on the shorter streamwise scale corresponding to $2\pi/(\alpha_{TS}^* - \alpha_w^*)$, resulting in a cancellation of contributions from adjacent source locations. The integral is then end-point dominated, implying that the only receptivity occurs at the extremes of the surface inhomogeneity distribution. To understand this point more clearly, one may note that the wide, isolated strip considered before may also be viewed as a special case of the spatially-periodic distribution, having a zero wavenumber throughout the interior region. Recall that Fig. (3b) showed how the receptivity in this case is nearly localized to the end-points of the suction strip.

Another way to look at the spatially-periodic case is to consider it in the context of the wave amplitude equation (2.13). From this viewpoint, when $\alpha_w - \alpha_{TS}$ is $O(1)$, the particular solution of (2.13) (which is proportional to the wall-disturbance phase Θ_w) is effectively decoupled from the eigenmode solution (which is proportional to the T-S phase Θ_{TS}), and, therefore, cannot transfer energy to the instability wave. In the other extreme, when the two wavenumbers are exactly equal, which can only occur at a neutral station since we are considering completely periodic surface disturbances, contributions from the adjacent locations are in phase with each other, thus summing up to very high levels of receptivity. Of course, the slow variations in the boundary-layer profile change the instability wavenumber gradually, thereby making the two phases uncorrelated at far away distances. In other words, the forcing is detuned with respect to the instability wave far

upstream of the neutral station; it is locally resonant near the neutral station and detuned again far enough downstream.

The length scale over which the resonance lasts, and, hence, over which the local contributions add up directly, would determine precisely how much larger the effective coupling coefficient is when compared to the localized case. The magnitude of this ratio can easily be seen to be of $O(R_{l.b.}^{3/8})$ by inspecting the asymptotic approximation

$$C_{TS}^{(j)} = \frac{\sqrt{2}\, E_q(Y; \omega, R_{l.b.})\, \Lambda^{(j)}(\omega, R_{l.b.})}{\sqrt{i\left(\frac{d\alpha_{TS}}{dR} - \frac{d\alpha_w}{dR}\right)_{R=R_{l.b.}}}}\,, \qquad (2.16)$$

obtained by exploiting the local stationarity of the integrand phase, $\Theta_w - \Theta_{TS}$, at the resonance location $R = R_{l.b.}$ [42]. The dispersion factor $\left(\frac{d\alpha_w}{dR} - \frac{d\alpha_{TS}}{dR}\right)_{R=R_{l.b.}}$ is essentially a measure of how fast the forcing becomes out of "tune" with the eigenmode. As discussed in Ref. 42, the imaginary part of $d\alpha_{TS}/dR$ is larger than its real part for all frequencies, thereby suggesting that the detuning effect is primarily due to growth rate variation in the vicinity of the neutral curve as against the variation in the phase velocity. As mentioned at the beginning of this section, the above ideas can be put on a more rigorous basis, which also permits the analysis of more general near-resonant geometries (corresponding to arbitrary modulations of the periodic forcing on the resonance scale), and the reader is refered to Ref. 42 for the details of this analysis. Finally, one may also point out that since the result (2.16) is independent of the nature of the surface-nonuniformity, it also confirms, as well as explains, the more recent computations by Crouch (Ref. 5), where he found the receptivity due to surface waviness to be "two orders of magnitude" larger than that due to an isolated roughness element, as against his earlier findings (Ref. 6) that the receptivity is comparable in both cases.

We now consider the question of numerically solving the wave amplitude equation for this case. A crucial difference here from the discrete configurations examined previously is that they all had a finite support, i.e., a definite streamwise origin, which simplified the specification of an initial condition for the numerical integration. However, the periodic

distributions have an infinite support, and in order to avoid starting the integration right from the leading edge, one has to specify an appropriate initial condition at some finite distance downstream.

Tam[27], who examined the acoustic receptivity in the absence of any surface disturbance, utilized a homogeneous initial condition for solving the amplitude equation. However, the acoustic wavenumber is largely different from the instability wavenumber in low-speed flows. Hence, the resonance condition is never satisfied, and as argued in the previous paragraph, there would be little resultant receptivity in the entire region of integration. Whatever small amplitudes one finds by the numerical integration process would essentially be dominated by the end-point contributions. This only suggests the inappropriateness of the numerical treatment, since the inflow location was chosen on a completely artificial basis. Furthermore, setting the initial condition to zero automatically gives rise to both the particular and the eigenmode solutions right at the inflow boundary, each having the same (initial) amplitude but opposite phase. Once generated, these two solutions remain decoupled from each other, effectively propagating independently throughout the region of integration. Thus, Tam's argument that the receptivity only occurs at the start of integration is correct mathematically but not physically, having stemmed from the unphysical initial conditions as discussed above. One should also note that, in his case, the amplitude of the particular solution is essentially equivalent to the amplitude of the free-stream disturbance, thus being independent of the local Reynolds number. Moreover, since Tam imposed the initial condition at $R \approx 378$, i.e., fairly close to the neutral location ($R = 576$) of the frequency being considered ($f = 56 \times 10^{-6}$), the inflow-generated T-S wave did not decay much (by a factor of $\approx 1/5$) before reaching the neutral station. Hence, the calculated coupling coefficients were found to be $O(1)$, and also to be insensitive to small changes in the inflow Reynolds number.

In our case, provided the resonance condition is satisfied exactly, or nearly so, the receptivity is confined to a relatively short region in the interior, and we adopt the viewpoint that, as long as the inflow location is chosen to be sufficiently far upstream

of the lower branch, the physical decay of the instability wave in the region upstream of $R_{l.b.}$ also serves to damp out any errors due to inappropriateness of the initial condition. Thus, we found that the somewhat ill-founded homogeneous initial condition yields very good agreement with the results obtained from the more rational inhomogeneous initial condition corresponding to a nonzero particular solution but a zero eigenmode.

Figure 5a shows the variation of the wave amplitude in the wall-admittance problem for the resonant distribution corresponding to $\alpha_w = \alpha_{TS}$ at $R = R_{l.b.}$ for $f = 20 \times 10^{-6}$. The cumulative contribution to the effective coupling coefficient, as well as its rate of change with respect to the local Reynolds number, are plotted in Figs. 5b and 5c, respectively. The lower and upper branch locations at this frequency are indicated by circles in Figs. 5a-5c. Note that the ordinate in Fig. (5a) corresponds to the total amplitude, i.e., sum of both the particular and homogeneous solutions. The numerical calculation in this case essentially involves integrating across the resonance region, where both solutions are linearly dependent by virtue of having an identical phase variation to the leading order. This implies that a unique decomposition of the total solution into its particular and homogeneous components cannot be accomplished in a sensible manner, and an attempt to force this separation (as in Ref. 5, where the receptivity due to surface waviness was examined) may result in misleading conclusions. This, we believe, is the reason for the observed overshoots in Ref. 5 in the amplitude of the homogeneous solution in vicinity of the lower branch location, although on physical grounds one would expect a spatially-monotonic transfer of energy to the instability wave. It should be noted that the spatially-periodic problem leads only to a transient resonance, and, therefore, no singularity is expected in the total solution. Therefore, separating the particular and homogeneous solutions leads to artificial spikes in each component, each of them having little physical meaning.

Figure 5b shows that the magnitude of the effective coupling coefficient increases rapidly in vicinity of $R_{l.b.}$ (≈ 1037, indicated by an open circle in the figure), and remains nearly constant in most of the unstable region. More specifically, it is seen from Fig. 5c that the dominating contributions to $|C^{(j)}|$ are produced in a fairly small Reynolds-number

range, of approximately 800-1200. Similar behaviour was also observed at other values of the frequency parameter.

Figure 6a shows the effective coupling coefficient, $C^{(j)}$, after being normalized by the wall suction parameter $\epsilon_w^{(1)}$, as a function of the Reynolds number $R_{\lambda_w^*}$ based on the wavelength of the wall suction distribution. Analogous results for the wall-admittance problem are shown in Fig. 6b. In both figures, results are plotted for frequencies ranging from $f = 20 \times 10^{-6}$ to $f = 55 \times 10^{-6}$. The corresponding N-factors are between approximately 12 and 4, and, hence, the above range covers the frequencies of interest in both laboratory and flight applications. Figures 6a-b show that the receptivity at each frequency is mainly concentrated in a narrow range of wavelengths, with the effective coupling coefficient dropping off in a rapid but nearly symmetric manner away from the peak location. In view of the discussion in the previous paragraphs, it is not surprising that the wavelength corresponding to the maximum receptivity is equal to the T-S wavelength at the lower branch location.

The rapid change in $|C^{(j)}|$ in the vicinity of the resonant wavelength indicates the rather dramatic effect receptivity might have upon the performance of the LFC system under certain circumstances. In particular, if the free-stream disturbances are dominated by the engine noise, in particular its discrete components corresponding, for example, to the harmonics of the blade-passing frequency, then it becomes imperative to avoid suction-strip spacings which are integer multiples of the neutral T-S wavelength at such frequencies. If sufficient attention is not paid to these issues during the design process, slight variations in the unit Reynolds number could increase the receptivity by an order of magnitude, as shown by figures 6a and 6b.

The envelopes of the curves in Figs. 6a,b demonstrate how the maximum possible receptivity varies with the free-stream disturbance frequency, or alternatively with the wavelength of the surface nonuniformity distribution. For the purpose of comparison, we have also shown the stationary phase result (2.16) as the dashed curve in these figures. As one can see, there is an excellent agreement between the two results in the entire range

25

of frequencies. One may observe that the maximum receptivity increases fairly rapidly as the frequency parameter decreases. However, since the shape of the individual curves appears to insensitive to the value of f, perhaps a more appropriate way to characterize this type of receptivity would be to consider the effective couping coefficient as a function of the detuning of the forcing wavenumber with respect to the resonant value. In fact, considering the success of the stationary phase result, one could also rescale the ordinate by utilizing simple order of magnitude estimates obtained through (2.16) used in conjunction with the standard high Reynolds number asymptotic theory of T-S waves[42]. Figures 7a,b show the results from Figs. 6a,b replotted with the new absissca corresponding to the wavenumber detuning parameter expressed as a percentage, and the ordinate being scaled by the coupling coefficient in the zero detuning case. It is clear that, in each case, the different curves have nearly collapsed onto each other, indicating that the dependence of the coupling coefficient on the detuning parameter is practically independent of the frequency parameter in the range of interest.

4. SUMMARY AND CONCLUDING REMARKS

In this paper, we have examined a simplified problem related to the acoustic receptivity of boundary layers over airfoil surfaces equipped with laminar flow control systems. This model problem involves the generation of instability waves in a non-compact region of short-scale variations in the surface suction velocity and/or admittance of the porous surface. In particular, it was shown how the results for semi-compact or localized regions of instability, i.e., regions which are comparable to the instability wavelength in their streamwise extent, can be conveniently extended to more general situations. The principal conclusions of this study are summarized below:

1. The same underlying physics behind the wavelength reduction process in localized receptivity problems also applies in the distributed case.

2. The major difference between the localized and distributed receptivity problems is related to the magnitudes of the respective coupling coefficients, which are much larger in the latter case, by a factor of $O(R_{l.b.}^{3/8})$ based on asymptotic arguments.

3. Most of the receptivity in the distributed case still occurs in a relatively short region, of length $O(R_{l.b.}^{3/8} \ell^*)$, in the vicinity of the lower branch of the neutral stability curve. This also implies that non-parallel effects can, again, be neglected to the leading order in modelling this class of receptivity problems.

4. The receptivity due to spatially homogeneous distributions of surface suction and admittance is dominated by a narrow band of Fourier harmonics, which involve a detuning of less than about 10% with respect to the neutral instability wavenumber at the lower branch location.

5. The functional variation of the effective coupling coefficient with respect to the detuning parameter is nearly independent of the frequency of the external disturbance.

Having stated the conclusions, we would like to summarize the limitations of the present results, and also suggest possible ways to overcome these limitations. As mentioned before, the limitation to weak suction and admittance variations is mainly a theoretical one, and, not likely to impede the application of the theory to real world problems. Perhaps the principal limitation of the results in Section 3 stems from neglecting the role of surface nonuniformities in modifying the stability of the base flow and in downstream scattering of the instability waves produced by upstream variations in wall-suction or admittance. Much of the stability modification really comes from the mean (spatially averaged) suction level, since the accompanying variations only lead to an alternating pattern of stabilization (in regions where the suction is larger than the mean) and destabilization (where there is no suction or the suction level is below the mean), the net effect of which is of a higher order as far as stability properties are concerned. However, these variations, in addition to producing receptivity, also scatter a small fraction of the instability waves coming from upstream. The relative effect of these neglected phenomena is locally of $O(\epsilon_w^{(j)})$, and their neglect can, therefore, be justified even on the longer length scale of the receptivity process by placing additional restrictions on the magnitudes of the surface suction and admittance parameters. For practical applications, however, the accuracy of the coupling coefficients

may be affected somewhat significantly by the errors introduced by these approximations, especially the one related to the influence of mean suction.

Fortunately, the basic framework described in Section 2 appears to be flexible enough to incorporate both of these effects in a relatively straightforward fashion. The enhanced stability due to the use of suction may be accounted for by incorporating the mean suction into the base flow Ψ_0 and computing the relevant quantities (such as α_{TS} and $\Lambda^{(j)}$) on the basis of this modified boundary-layer profile. Due to the nonsimilar nature of Ψ_0, however, this would also mean repeating the entire calculation, including the efficiency functions $\Lambda^{(j)}$ for each configuration of interest. The issue of instability wave scattering by surface nonuniformities has just begun to be analyzed in recent years, although it had previously been looked into in great detail in relation to the scattering of radio waves (and also acoustic waves) by distributed surface topography. Again, it would be possible to incorporate the scattering coefficients from a local calculation, such as that of Zhang and Kerschen[43] for the wall-admittance problem, into the amplitude evolution equation along much the same lines as the present generalization of the instability wave "production" from local coupling coefficients to larger distances.

Finally, even though the nonparallel effects are asymptotically small, and are expected to be numerically small as well, if and when they do become significant in a numerical sense, they can be accommodated fairly easily by using results from the usual weakly-nonparallel theory. In such a case, one simply needs to replace the quasiparallel phase function, Θ_{TS}, in (2.12) with its nonparallel counterpart.

Overall, the present analysis provides a convenient tool to study the receptivity in arbitrary nonlocalized geometries, instead of just quasiperiodic distributions. Note that the problem of receptivity due to wall suction/admittance variations is somewhat simpler in that one may assume a complete knowledge about the respective distributions for estimating the receptivity. Moreover, due to the multiple strip/slot configurations, the spatial spectra involved are discrete in nature. In contrast, the problem of roughness-induced receptivity involves both systematic distortions of the surface (related to surface joints and

fastenings) and random ones originating during the manufacturing process itself, or arising during operation (e.g., skin erosion, insect debris, etc.[28]). In addition, the spectrum of surface imperfections inevitably include both discrete and continuous components. The deterministic part of this problem can be handled along much the same lines as here; however, the random component will require accounting for the stochastic nature of the forcing. Understanding the receptivity process in wide-band, as well as random, disturbance environments is indeed a daunting task, but one for which the prognosis appears quite promising at the present time, especially in the experimental direction; see Kendall[44]. As a first step towards addressing such issues theoretically, we have considered the interactions involving random surface-disturbance fields, and the results of this investigation are being reported in a separate paper.

Acknowledgements

References

1. Goldstein, M.E., "Scattering of Acoustic Waves into Tollmien-Schlichting Waves by Small Streamwise Variations in Surface Geometry," *J. Fluid Mech.*, Vol. 154, pp. 509-529, 1985.

2. Ruban, A.I., "On the Generation of Tollmien-Schlichting Waves by Sound," Transl. in *Fluid Dyn.*, Vol. 19, pp. 709-16, 1985.

3. Kerschen, E.J. and Choudhari, Meelan, "Boundary layer receptivity due to the interaction of free-stream acoustic waves with rapid variations in wall suction and admittance distributions", *Bull. Am. Phys. Soc.*, 1985; see also: Choudhari, Meelan, "Boundary Layer Receptivity Mechanisms Relevant to Laminar Flow Control," Ph.D. dissertation, University of Arizona, 1990.

4. Choudhari, Meelan and Streett, C.L., "A Finite Reynolds Number Approach for the Prediction of Boundary Layer Receptivity in Localized Regions," NASA TM-102781, Jan. 1991.

5. Crouch J.D., "Initiation of Boundary-Layer Disturbances by Nonlinear Mode Interactions," Boundary Layer Stability and Transition to Turbulence, Ed. Reda *et al*, FED-Vol. 114, ASME, N.Y., pp. 63-68, 1991.

6. Crouch J.D., "A Nonlinear Mode Interaction Model for Boundary Layer Receptivity," *Bull. APS*, Vol. 35, No. 10, p. 2262, 1991.

7. Heinrich, R.A.E, Choudhari, Meelan and Kerschen, E.J., "A comparison of Boundary Layer Receptivity Mechanisms," AIAA Paper 88-3758, 1988.

8. Kerschen, E.J., "Boundary Layer Receptivity," AIAA Paper 89-1109, 1989.

9. Bodonyi, R.J., Welch, W.J.C., Duck, P.W. and Tadjfar, M., "A Numerical Study of the Interaction between Unsteady Free-Stream Disturbances and Localized Variations in Surface Geometry," *J. Fluid Mech.*, Vol. 209, pp. 285-308, 1989.

10. Choudhari, Meelan and Kerschen, E.J., "Instability Wave Patterns Generated by Interaction of Sound Waves with Three-Dimensional Wall Suction or Roughness," AIAA Paper 90-0119, 1990.

11. Choudhari, Meelan and Kerschen, E.J., "Boundary Layer Receptivity due to Three-Dimensional Convected Gusts," Proceedings of ICASE/NASA LaRC Instability and Transition Workshop, Springer-Verlag, 1990.

12. Choudhari, Meelan and Kerschen, E.J., "Instability Wave Patterns Generated by Interaction of Sound Waves with 3-D Wall Suction or Roughness," AIAA Paper 90-0119, 1990.

13. Denier, J.P., Hall, P. and Seddougi, S., "On the Receptivity Problem for the Gortler Vortices: Vortex Motions Induced by Wall Roughness", ICASE Report 90-31, 1990.

14. Reed, H. L., Lin, N. and Saric, W. S., "Boundary Layer Receptivity to Sound: Navier-Stokes Computations," *Appl. Mech. Rev.*, Vol. 43, no. 5, Part 2, May 1990, pp. S175-S180.

15. Choudhari, M., Ng, L. and Streett, C. L., "A General Approach for the Prediction of Boundary Layer Receptivity due to Short-Scale Variations in Surface Boundary Conditions," Proc. Conf. on Boundary Layer Transition and Control, Cambridge, UK, April 1991.

31

16. Kerschen, E. J., "Linear and Nonlinear Receptivity to Vortical Free-Stream Disturbances," Boundary Layer Stability and Transition to Turbulence, Ed. Reda *et al*, FED-Vol. 114, ASME, N.Y., pp. 43-48, 1991.

17. Pal, A., Bower, W. W. and Meyer, G. H., "A Parametric Study of Boundary Layer Receptivity for an Acoustic Wave/Porous Plate Interaction," Boundary Layer Stability and Transition to Turbulence, Ed. Reda *et al*, FED-Vol. 114, ASME, N.Y., pp. 77-82, 1991.

18. Shapiro, P. J., "The influence of sound upon laminar boundary layer instability," MIT Acoustics and Vibration Lab. Rep. 83458-83560-1, 1977.

19. Aizin, L. B. and Polyakov, M. F., "Acoustic Generation of Tollmien-Schlichting Waves over Local Unevenness of Surface Immersed in Stream (in Russian)," Preprint 17, Akad. Nauk USSR, Siberian Div., Inst. Theor. Appl. Mech., Novosibirsk, 1979.

20. Wlezien, R. W., Parekh, D. E. and Island, T. C., "Measurements of Acoustic Receptivity at Leading Edges and Porous Strips," Proc. 11th U.S. Natl. Congress Appl. Mech., Tucson, May 1990.

21. Saric, W., Hoos J. A. and Radeztsky, R. H., "Boundary Layer Receptivity of Sound with Roughness," Boundary Layer Stability and Transition to Turbulence, Ed. Reda *et al*, FED-Vol. 114, ASME, N.Y., pp. 17-22, 1991.

22. Nishioka, M. and Morkovin, M. V., "Boundary Layer Receptivity to Unsteady Pressure Gradients: Experiments and Overview," *J. Fluid Mech.*, Vol. 171, pp. 219-261, 1986.

23. Goldstein, M. E. and Hultgren, L. S., "Boundary-layer Receptivity to Long-Wave Free-Stream Disturbances," *Ann. Rev. Fluid Mech.*, Vol. 21, pp. 137-166, 1989.

24. Kerschen, E.J., "Boundary Layer Receptivity Theory," Proc. 11th U.S. Natl. Congress Appl. Mech., Tucson, May 1990.

25. Hall, P., "Görtler Vortices in Growing Boundary Layers: The Leading Edge Receptivity Problem, Linear Growth and the Nonlinear Breakdown Stage," ICASE Report 89-81, 1989.

26. Choudhari, Meelan and Streett, C.L., "Boundary Layer Receptivity Phenomena in Three-Dimensional and High-Speed Boundary Layers," AIAA Paper 90-5258, 1990.

27. Tam, C.K.W., "The Excitation of Tollmien-Schlichting Waves in Low Subsonic Boundary Layers by Free-Stream Sound Waves," *J. Fluid Mech.*, Vol. 109, pp. 483-501, 1981.

28. Braslow, A. L. and M. C. Fischer, "Design Considerations for Application of Laminar Flow Control Systems to Transport Aircraft," AGARD-R-723, pp. 4.1-4.27, 1985.

29. Wagner, R. D., Bartlett, D. W. and Maddalon, D. V., "Laminar Flow Control is Maturing," *Aerospace America*, pp. 20-24, Jan. 1988.

30. Saric, W. S. and Reed, H. L., "Effect of Suction and Weak Mass Injection on Boundary Layer Transition," *AIAA J.*, Vol. 24, no. 3, pp. 383-389, March 1986.

31. Nayfeh, A. H. and El-Hady N. M., "An Evaluation of Suction through Porous Strips for Laminar Flow Control," *AIAA Paper.* 79-1494, 1979.

32. Reynolds, G. A. and Saric, W. S., "Experiments on the Stability of the Flat Plate Boundary Layer with Suction," *AIAA J.*, Vol. 24, no. 2, pp. 202-207, Jan. 1985.

33. Reed, H. L. and Nayfeh, A. H., "Stability of Flow over Plates with Porous Suction Strips," AIAA Paper 81-1280, 1981. See also, "Numerical Perturbation Technique for Stability of Flat-Plate Boundary Layers with Suction," *AIAA Jl.*, Vol. 24, no. 2, pp. 208-214, 1985.

34. Masad J., and Nayfeh, A. H., "Laminar Flow Control of Subsonic Boundary Layers by Suction and Heat-Transfer Strips," Accepted for publication in *Phys. Fluids A*, 1992.

35. El-Hady, N., "Effect of Suction on Controlling the Secondary Instability of Boundary Layers," *Phys. Fluids A*, Vol. 3, no. 3, pp. 393-402, March 1991.

36. El-Hady, N., "Secondary Instability of High-Speed Flows and the Influence of Wall Cooling and Suction," *AIAA Paper*, 91-1647, 1991.

37. Masad J., and Nayfeh, A. H., "Effect of Suction on the Subharmonic Instability of Compressible Boundary Layers," *Phys. Fluids A*, Vol. 3, no. 9, pp. 2179-2190, 1991.

38. Saric, W. and Nayfeh, A. H. "Nonparallel Stability of Boundary Layer Flows," *Phys. Fluids*, Vol. 18, No. 8, pp. 945-950, 1975.

39. Gaster, M., "On the Generation of Spatially Growing Waves in a Boundary Layer," *J. Fluid Mech.*, Vol. 22, pp. 433-441, 1965.

40. Tumin and Federov, *Proc. IUTAM Symp. on Laminar-Turbulent Transition*, Novosibirsk, USSR, 1985.

41. Ashpis, D. and Reshotko, E., "The Vibrating Ribbon Problem Revisited," *J. Fluid Mech.*, Vol. 213, pp. 531-547, 1990.

42. Choudhari, Meelan, "Boundary-Layer Receptivity due to Distributed Surface Imperfections of a Deterministic or Random Nature," NASA CR-4439, May 1992.

43. Zhang, H. and Kerschen, E. J, "Scattering of Tollmien-Schlichting Waves by Short-Scale Variations in Wall Admittance," *Bull. Am. Phys. Soc.*, Vol. 36, No. 10, 1991, p. 2618.

44. Kendall, J. M., "Studies on Laminar Boundary Layer Receptivity to Free-Stream Turbulence near a Leading Edge," Boundary Layer Stability and Transition to Turbulence, Ed. Reda *et al*, FED-Vol. 114, ASME, N.Y., pp. 17-22, 1991; see also: *Bull. Am. Phys. Soc.*, Vol. 36, No. 10, 1991, p. 2619.

Table 1

Receptivity due to multiple strip configurations

case no.	region of suction	no. of strips	type of distribution	$|C^{(j)}|$
(i)	$R < R_{l.b.}$	12	uniform = 1.0	902
(ii)	$R_{l.b.} < R < R_{u.b.}$	48	uniform = 1.0	829
(iii)	$R < R_{u.b.}$	60	uniform = 1.0	1639
(iv)	$R_{l.b.} < R < R_{u.b.}$	48	concentrated near neutral locations; 1.2 in outer 3rds, 0.6 in middle 3rd.	997
(v)	$R_{l.b.} < R < R_{u.b.}$	48	concentrated in the middle of the unstable region; 1.5 in middle 3rd, 0.75 in outer 3rds.	620
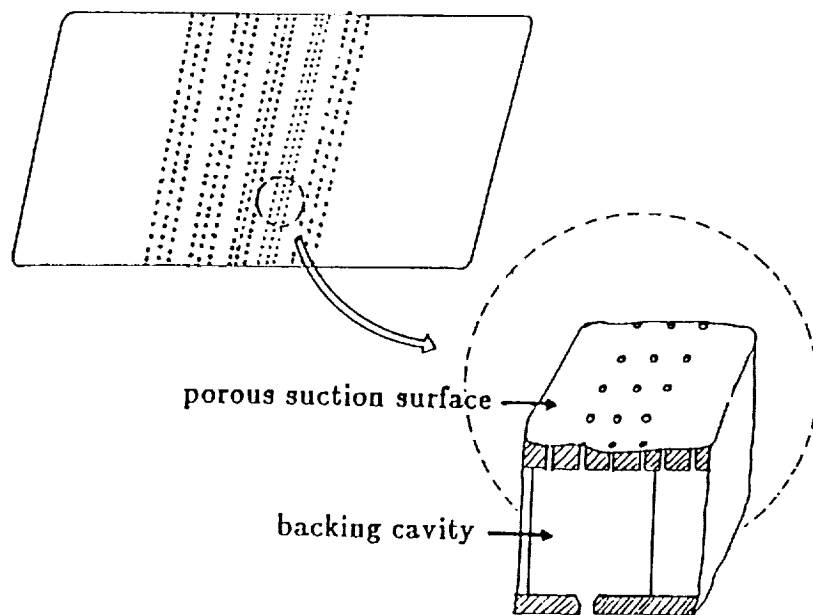
Fig. 1a Schematic of the laminar flow control system using distributed suction through a porous surface.
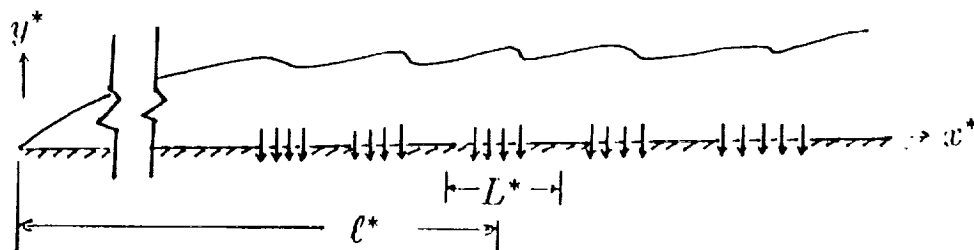
Fig. 1b Sketch of the coordinate system.
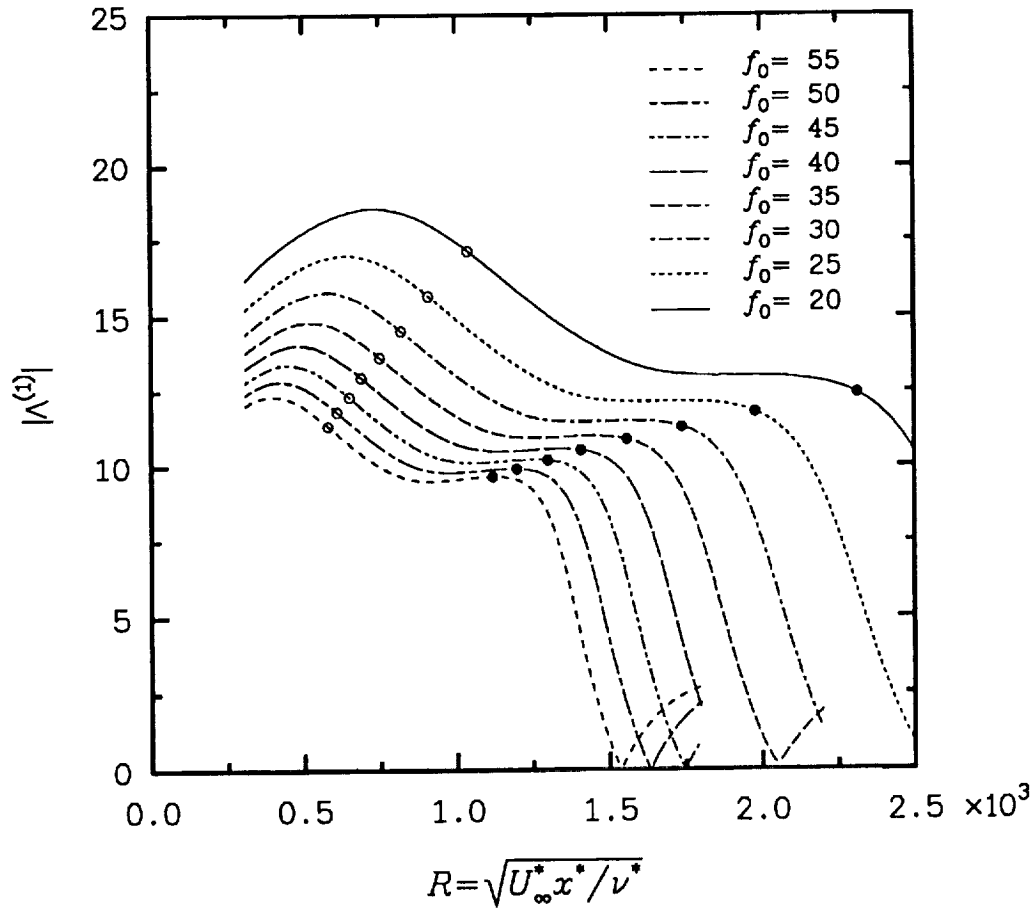
36
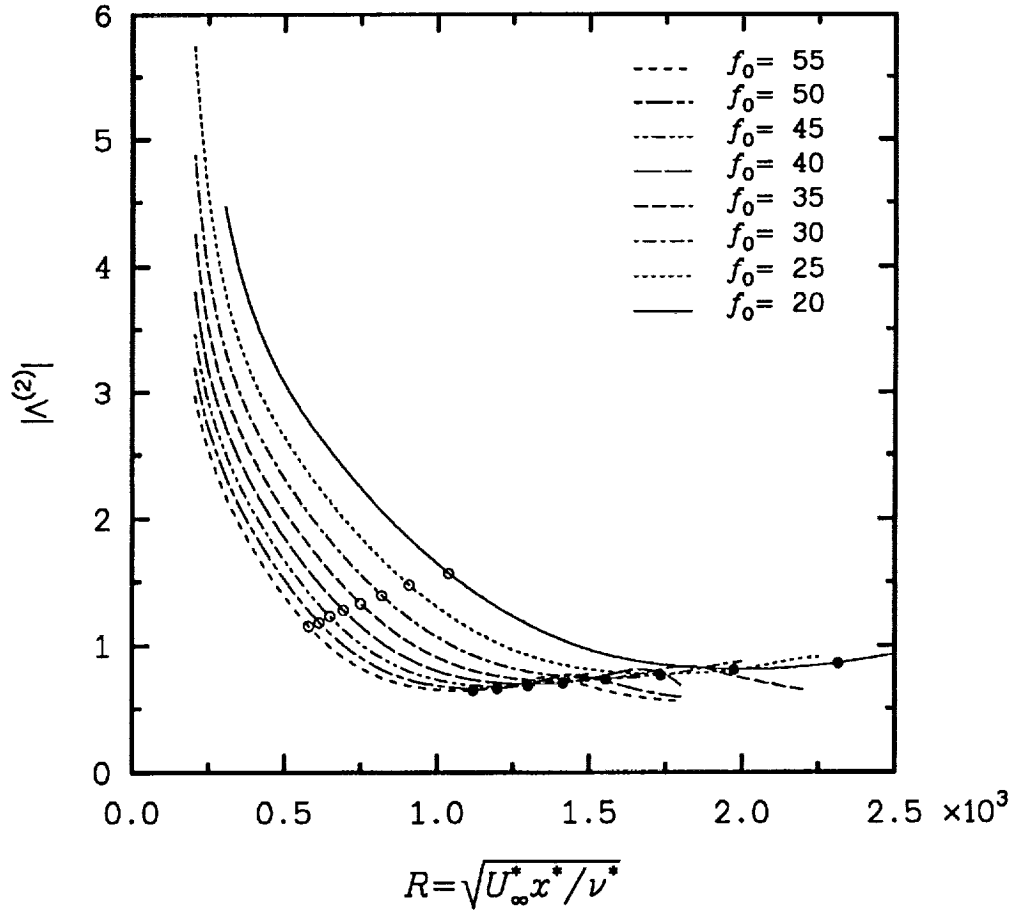
Fig. 2   Magnitudes of the efficiency functions $\Lambda^{(j)}$, $j=1-2$

from Eqs. (2.9-2.12) as functions of the wall inhomogeneity location

R with $f_0 = 10^6 \times \omega^* \nu^*/U_\infty^{*2}$ as a parameter.
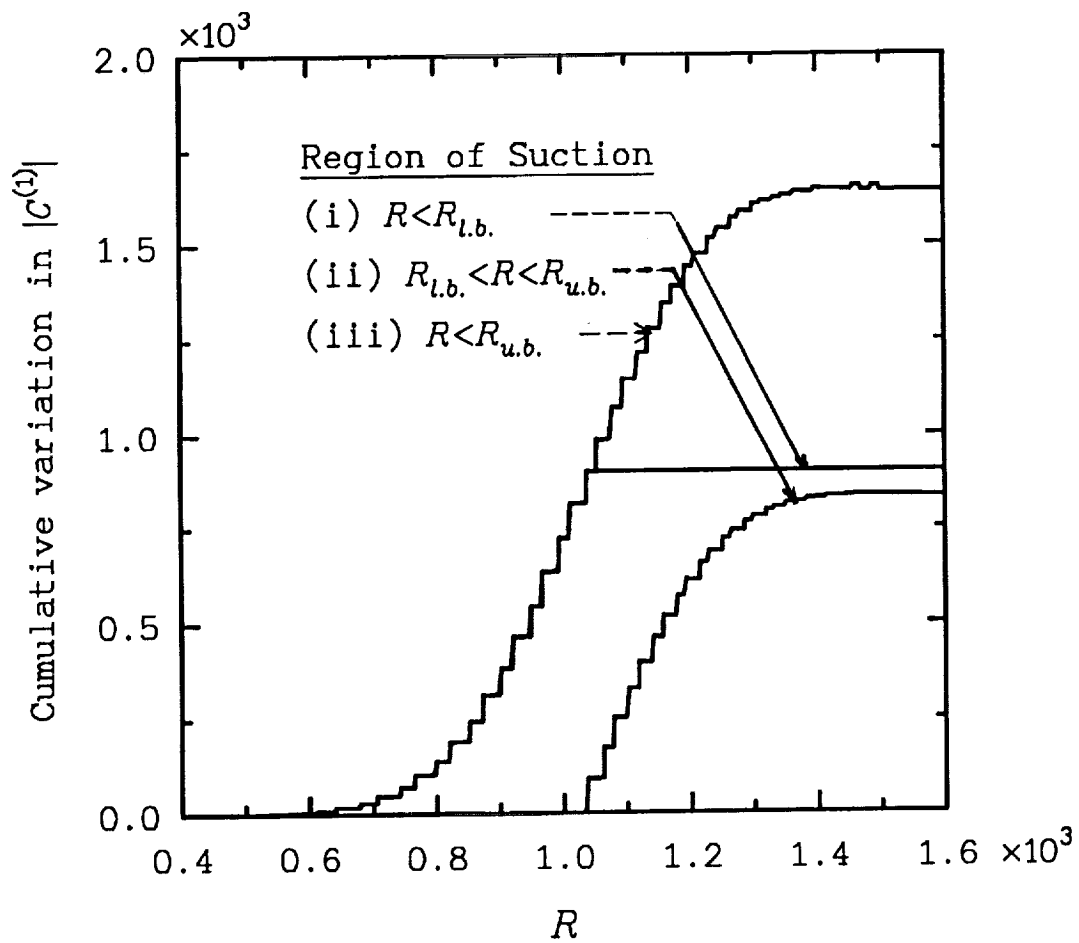
(a) Receptivity due to wall suction variation ($j=1$)

37

Fig. 2   Magnitudes of the efficiency functions $\Lambda^{(j)}$, j=1–2

from Eqs. (2.9–2.12) as functions of the wall inhomogeneity location

R with $f_0 = 10^6 \times \omega^* \nu^* / U_\infty^{*2}$ as a parameter.

(b) Receptivity due to wall admittance variation (j=2)

Fig. 4   Effect of suction in different parts of the airfoil chord
on the receptivity in a multiple strip suction configuration :
cumulative variation in the effective coupling coefficient $|C^{(1)}|$:
f=20 x 10^{-6}. $R_{l.b.}$≈1040, $R_{u.b.}$≈2315.
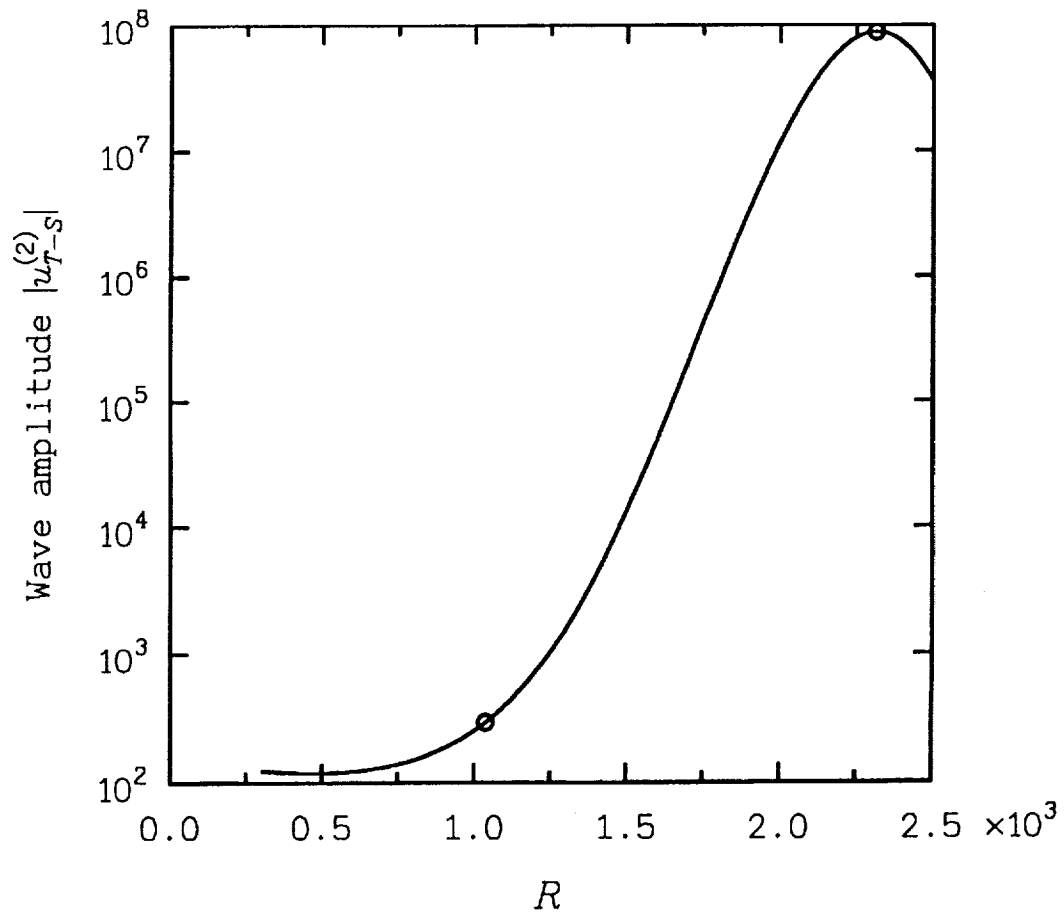
Fig. 5a   Receptivity induced by a periodic wall-admittance distribution

with a resonant wavenumber α_w corresponding to α_{T-S} ·

at the lower branch location, $R=R_{l.b.}$:

variation of the wave amplitude $u_{T-s}^{(2)}$ with respect to
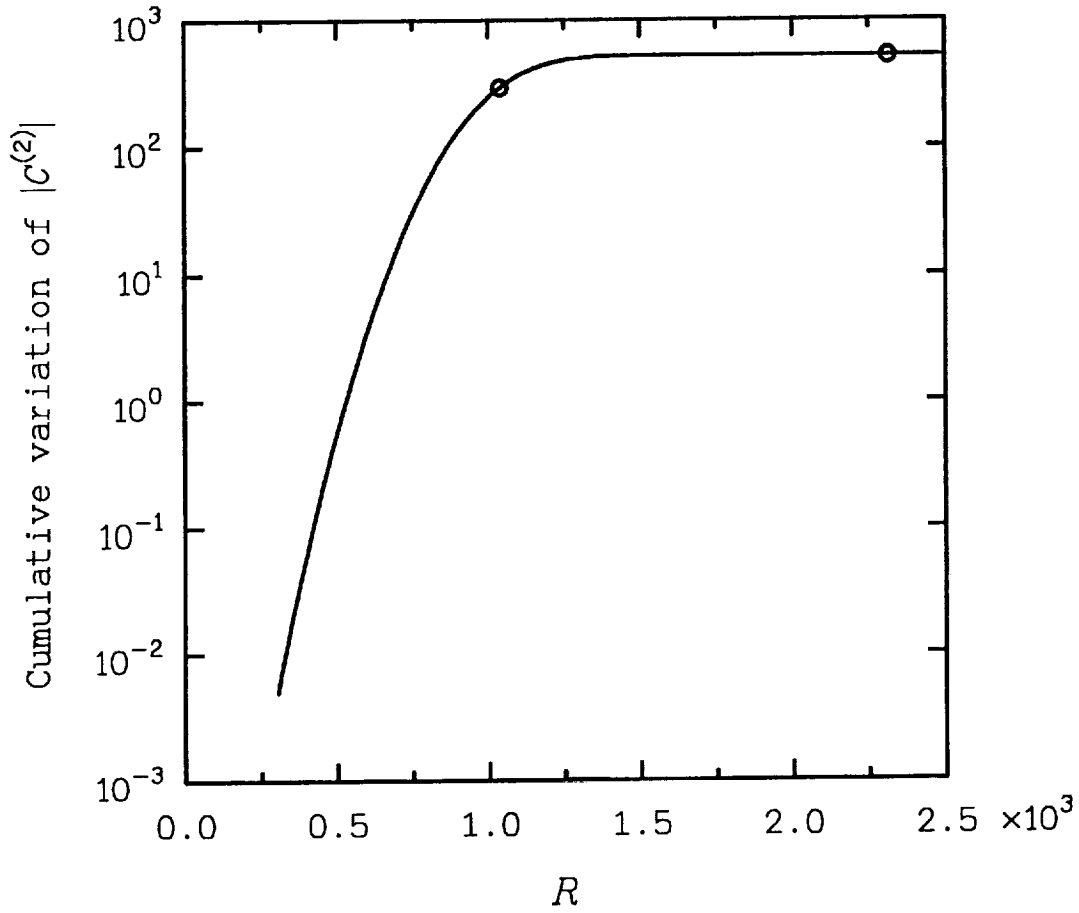
local Reynolds number, R; ($f=20 \times 10^{-6}$).

Fig. 5b   Receptivity induced by a periodic wall-admittance distribution

with a resonant wavenumber α_w corresponding to α_{T-S}

at the lower branch location, $R=R_{l.b.}$:

cumulative contribution to the effective coupling coefficient $|C^{(2)}|$ as

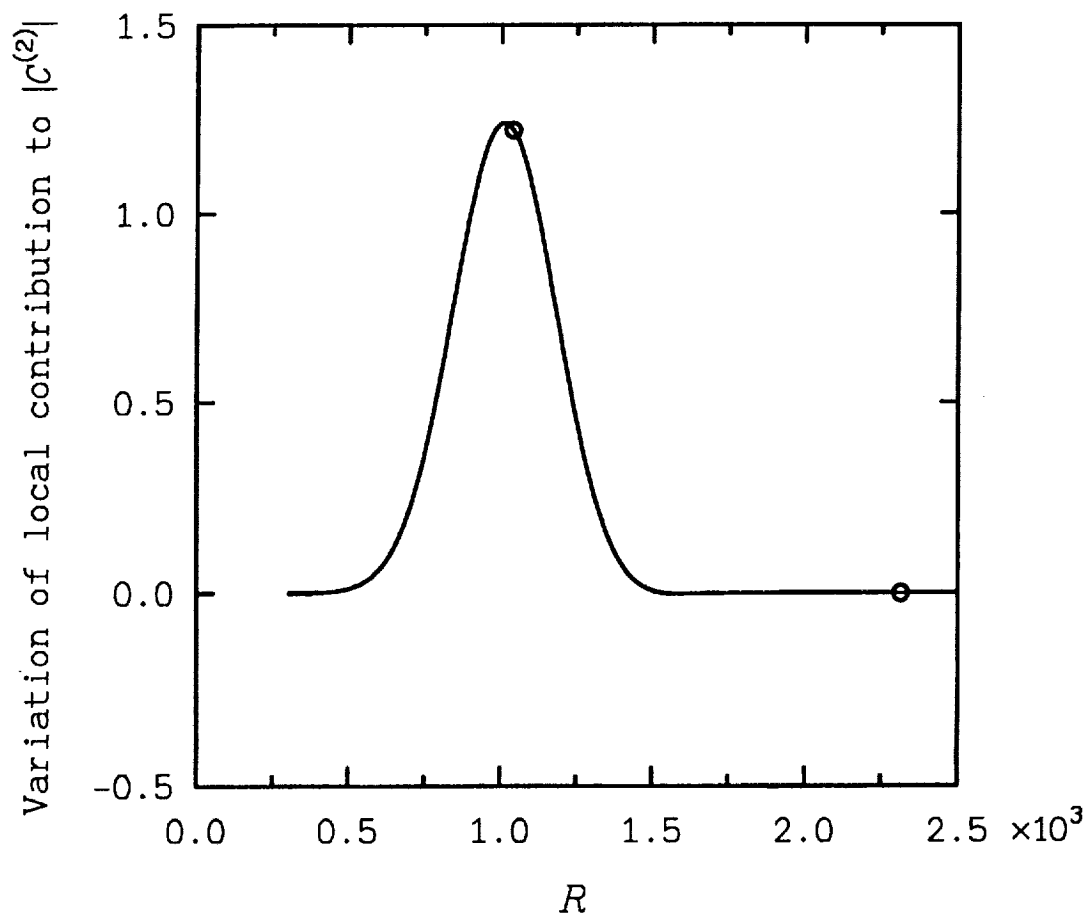a function of the local Reynolds number, R; ($f=20 \times 10^{-6}$).

Fig. 5c   Receptivity induced by a periodic wall-admittance distribution

with a resonant wavenumber α_w corresponding to α_{r-s} ·

at the lower branch location, $R=R_{l.b.}$:

local contribution to the effective coupling coefficient $|C^{(2)}|$ as

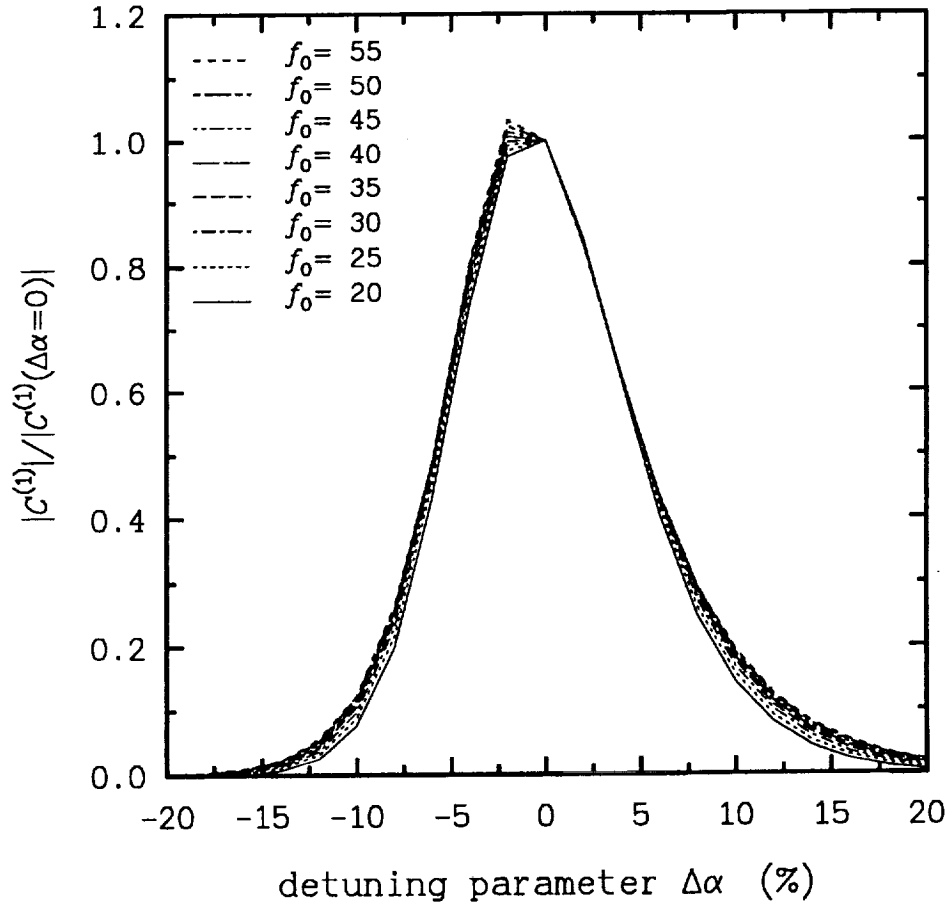a function of the local Reynolds number, R; ($f=20 \times 10^{-6}$).

Fig. 7 Receptivity induced by individual Fourier components
of spatially homogeneous surface disturbances :

The normalized effective coupling coefficient, $|C^{(1)}|/|C^{(1)}(\Delta\alpha=0)|$,
as a function of the wavenumber detuning parameter $\Delta\alpha$
expressed as a percentage.

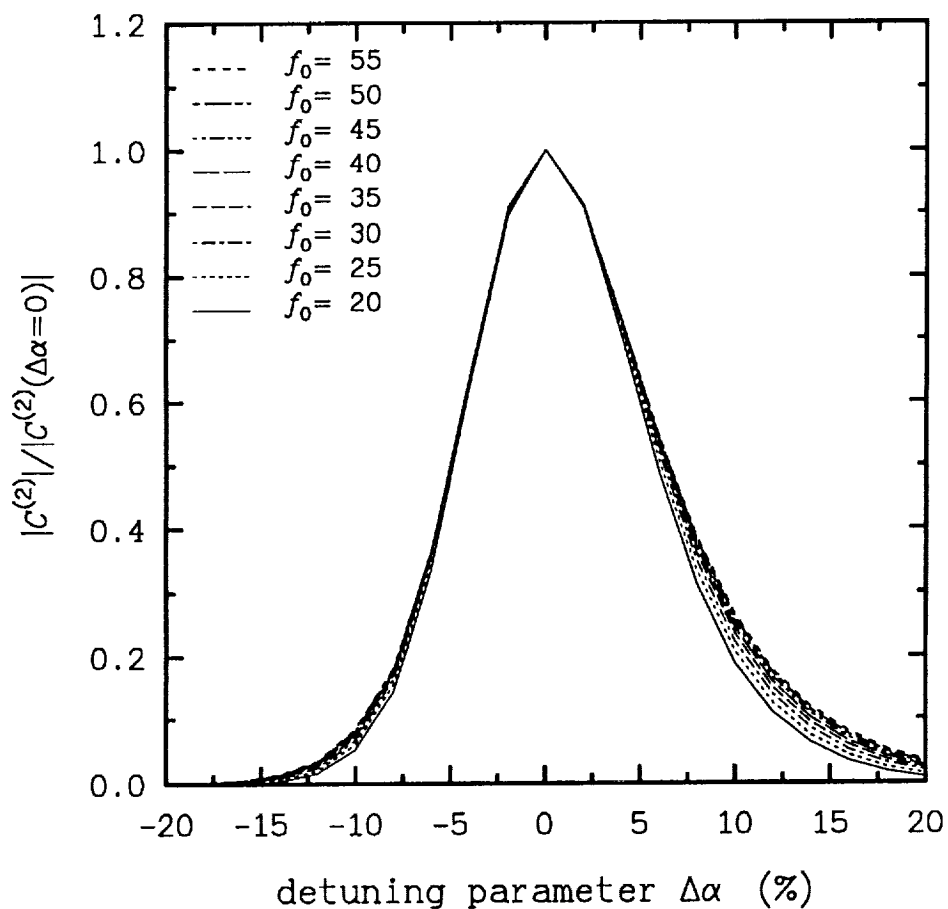(a) Receptivity due to wall suction variation

Fig. 7 Receptivity induced by individual Fourier components
of spatially homogeneous surface disturbances :

The normalized effective coupling coefficient, $|C^{(2)}|/|C^{(2)}(\Delta\alpha=0)|$,
as a function of the wavenumber detuning parameter $\Delta\alpha$
expressed as a percentage.

(b) Receptivity due to wall admittance variation

REPORT DOCUMENTATION PAGE

Public reporting burden for this collection of information is estimated to average 1 hour per response, including the time for reviewing instructions, searching existing data sources, gathering and maintaining the data needed, and completing and reviewing the collection of information. Send comments regarding this burden estimate or any other aspect of this collection of information, including suggestions for reducing this burden, to Washington Headquarters Services, Directorate for Information Operations and Reports, 1215 Jefferson Davis Highway, Suite 1204, Arlington, VA 22202-4302, and to the Office of Management and Budget, Paperwork Reduction Project (0704-0188), Washington, DC 20503.

1. AGENCY USE ONLY (Leave blank)	2. REPORT DATE May 1992	3. REPORT TYPE AND DATES COVERED Contractor Report

4. TITLE AND SUBTITLE Distributed Acoustic Receptivity in Laminar Flow Control Configurations	5. FUNDING NUMBERS C NAS1-18240
6. AUTHOR(S) Meelan Choudhari	WU 537-03-23-03

7. PERFORMING ORGANIZATION NAME(S) AND ADDRESS(ES) High Technology Corporation 28 Research Drive Hampton, VA 23666	8. PERFORMING ORGANIZATION REPORT NUMBER

9. SPONSORING / MONITORING AGENCY NAME(S) AND ADDRESS(ES) National Aeronautics and Space Administration Langley Research Center Hampton, VA 23665-5225	10. SPONSORING / MONITORING AGENCY REPORT NUMBER NASA CR-4438

11. SUPPLEMENTARY NOTES

Langley Technical Monitor: Craig L. Streett
Final Report

12a. DISTRIBUTION / AVAILABILITY STATEMENT Unclassified-Unlimited Subject Category 34	12b. DISTRIBUTION CODE

13. ABSTRACT (Maximum 200 words)   A model problem related to distributed receptivity to free-stream acoustic waves in laminar flow control (LFC) configuruations is studied, within the Orr-Sommerfeld framework,, by a suitable extension of the Goldstein-Ruban theory for receptivity due to localized distrubances on the airfoil surface. The results thus complement the earlier work on the receptivity produced by local variations in the surface suction and/or surface admittance. In particular, we show that the cumulative effect of the distributed receptivity can be substantially larger than that of a single, isolated suction strip or slot. Furthermore, even if the receptivity is spread out over very large distances, the most effective contributions come from a relatively short region in vicinity of the lower branch of the neutral stability curve. The length scale of this region is intermediate to that of the mean of these two length scales. Finally, it is found that the receptivity is effectively dominated by a narrow band of Fourier components from the wall-suction and admittance distributions, roughly corresponding to a detuning of less than ten percent with respect to the neutral instability wavenumber at the frequency under consideration. The results suggest that the drop-off in receptivity magnitudes away from the resonant wavenumber is nearly independent of the frequency parameter.

14. SUBJECT TERMS Receptivity, Transition, Boundary Layers	15. NUMBER OF PAGES 44
	16. PRICE CODE A03

17. SECURITY CLASSIFICATION OF REPORT Unclassified	18. SECURITY CLASSIFICATION OF THIS PAGE Unclassified	19. SECURITY CLASSIFICATION OF ABSTRACT	20. LIMITATION OF ABSTRACT

NSN 7540-01-280-5500